Crystallization Kinetics of Hard Spheres in Microgravity in the Coexistence Regime: Interactions between Growing Crystallites

Zhengdong Cheng,[1,*] P. M. Chaikin,[1] Jixiang Zhu,[2] W. B. Russel,[2] and W. V. Meyer[3]

[1]*Department of Physics, Princeton University, Princeton, New Jersey 08540*

[2]*Department of Chemical Engineering, Princeton University, Princeton, New Jersey 08540*

[3]*NCMR, NASA Glenn Research Center, Cleveland, Ohio 44135*

(Received 11 June 2001; published 14 December 2001)

The hard sphere disorder-order transition serves as the paradigm for crystallization. However, measurements of the crystallization kinetics for colloidal hard spheres in the coexistence regime are incomplete for early times and are affected by sedimentation. We use time resolved Bragg light scattering to characterize crystal nucleation and growth in a microgravity environment on the space shuttle. In contrast to the classical picture of the nucleation and growth of isolated crystallites, we find substantial coarsening of growing crystallites. We also observe dendritic growth and face-centered cubic as the stable structure.

DOI: 10.1103/PhysRevLett.88.015501 PACS numbers: 61.66.–f, 64.70.Dv, 81.10.–h, 82.70.Dd

Hard spheres, with an interaction energy of zero when separated and infinity when touching, are a model system for studying the structure and dynamics of liquids, crystals and glasses, as well as the phase transition between them [1–6]. The equilibrium phase diagram for hard spheres of uniform size depends only on the volume fraction ϕ occupied by the spheres. Computer simulation shows that liquid and crystalline phases coexist between 0.494 and 0.545. Below freezing, at $\phi_f = 0.494$, the liquid state is stable and above melting, at $\phi_m = 0.545$, the crystalline state is stable. At high concentrations, particles gain entropy by arranging themselves on a lattice to maximize interparticle distance and the local free volume. Studies of crystallization with colloids benefit from the convenient length scale (set by particle size, $\sim\mu$m) and time scale (set by particle diffusion, ~ms to days), which make light scattering techniques readily applicable.

In this Letter, we report the kinetics of colloidal hard sphere crystallization in the liquid-crystal coexistence regime in a microgravity environment. For particles not precisely density matched to the solvent, gravity can affect crystallization through sedimentation, convection, and viscous and compressional stresses. Among our quantitative observations are a dendritic growth instability, emergence of the face-centered cubic (fcc) structure as the equilibrium structure during annealing, and strong coarsening between crystallites during their growth stage. The latter observation negates the conventional view of a distinct growth phase followed by coarsening and points to interactions between the growing crystallites.

Classical theory for nucleation and growth was adapted by Russel [7] to hard sphere colloidal crystals and was extended and evaluated numerically by Ackerson and Schätzel [8]. Crystal growth is determined by coupling the Wilson-Frenkel growth law and pressure equilibrium at the crystal-liquid interface with a self-consistent concentration-diffusion field in the surrounding metastable liquid. The set of equations was solved numerically to determine the motion of the interface, the crystal size, densities, depletion zones, etc., as a function of elapsed time. Growth exponents were observed to first undergo long transients before approaching $1/2$ or 1, the long-time asymptotes expected for diffusion and reaction-limited growth, respectively. Consequences of this model are instructively illustrated also in [9] along with an analysis of the linear growth instability. Interactions between growing crystallites have not yet been considered.

On the experimental side, questions remain concerning the nature of the crystal growth, since consistent measurements in the coexistence regime are limited [10]. For example, low-angle light scattering studies in that regime [11,12] suggest that growth is proportional to the square root of the elapsed time, i.e., diffusion limited, while similar studies on smaller particles suggest growth exponents that vary between diffusion and interface limited growth [13]. In a recent study with PMMA-PHSA (polymethyl methacrylate-polyhydroxy stearic acid) spheres [14,15], crystallization below the melting concentration was compatible with the classic picture of sequential nucleation and the growth of *isolated* crystals. Palberg [10] reports the most complete set of data from a combination of small angle and Bragg scattering measurements, which yielded induction times and nucleation rates and roughly constant growth rates at short times. The initial growth rates, presumably before diffusion fields develop, are qualitatively consistent with the Wilson-Frenkel law, while the nucleation rates agree semiquantitatively with classical theory. However, the authors did not detect dendritic growth or coarsening at longer times.

Our recent microgravity experiments illustrated the role of gravity in crystallization kinetics [9,16,17]. A growth instability in coexistence, indicated by the dendritic shape of the crystallites, was observed photographically. It was later interpreted from a linear stability analysis of the growth equations for an isolated crystal. We report here the first quantitative microgravity study of colloidal hard sphere crystallization kinetics in coexistence.

The Physics of Hard Sphere Experiment (PHaSE) (for hardware details see [18–20]) flew aboard the Space Shuttle's Microgravity Science Laboratory twice in 1997 (STS-83 and STS-94). Eight samples can be loaded onto the test station sequentially through the rotation of a carousel. The index-matched glass sample cells contain 3.14 ml samples of PMMA-PHSA spheres, $2R = 600$ nm in diameter, suspended in a cis-decalin and tetralin mixture whose refractive index is matched to the spheres. For Bragg scattering, the optics produce an 8 mm diameter (e^{-2} intensity) collimated laser beam with a Gaussian profile. The 4 mW beam passes axially through the sample cell to illuminate the specimen. Light scattered into a Bragg pattern by the crystallizing PMMA spheres is focused by the hemispherical exit surface of the cell onto a concentric fluorescent screen. Mounted on the wall of the container is a 1032×1312 pixel charge-coupled device camera which, via a flat steering mirror, records an image of the fluorescent screen. A correction for the projection onto the camera and angular averaging yields the intensity I as a function of the wave number q.

The Bragg image is analyzed as follows [14]. The static structure factor of the metastable colloidal fluid can be described by the Percus-Yevick result $S_{PY}(q, \phi)$, where ϕ is the volume fraction of the fluid phase [3,21]. We estimate the product of the particle form factor $P(q)$ and the instrument factor $\alpha(q)$ by dividing the intensity $I(q, t = 0)$, measured immediately after shear melting, by $S_{PY}(q, \phi)$ at the overall volume fraction, $\alpha(q)P(q) = I(q, t)/S_{PY}(q, \phi)$. The structure factor $S(q, t)$ is then obtained (for $t > 0$) from $S(q, t) = I(q, t)/\alpha P(q)$, which represents the colloidal crystals and the fluid. The scattering from the crystal $S_c(q, t)$ is extracted by subtracting that from the fluid, $\beta(t)S_{PY}(q, \phi_L)$:

$$S_c(q, t) = S(q, t) - \beta(t)S_{PY}(q, \phi_L). \quad (1)$$

The fluid contribution as represented by the scale factor $\beta(t)$ is determined by decreasing $\beta(t)$ from unity until $S_c(q, t)$ approaches zero at small and large q. Here, ϕ_L, the volume fraction of the fluid regions in the sample, decreases with time as more and more spheres are converted from fluid to crystals. As crystallization progresses the structure of the crystals changes and $S_c(q, t)$ no longer falls to zero at our largest q value ($2qR < 9$) . We then choose $\beta(t)$ such that (i) at low q, $S_c \to 0$, (ii) $S(q)$ overlays fairly well at low q with the previous (time step) measurement, and (iii) the structure factor of the crystal is consistent with hexagonal planes of spheres with a stacking probability α. To assess the last factor, we calculated powder patterns from the expressions of Wilson [22] (see also [23]) and the orientational-averaging procedure described by Brindley and Méring [24]. A Gaussian function plus constant background was fit to the {111} peak [$qR \sim 7$ (see Fig. 1)] to estimate the maximum $q_m(t)$ and the half maximum width $\Delta q(t)$, as well as the low (q_1) and high (q_2) extent of the peak. The fraction $X(t)$ of the sample converted from fluid to crystal was calculated from

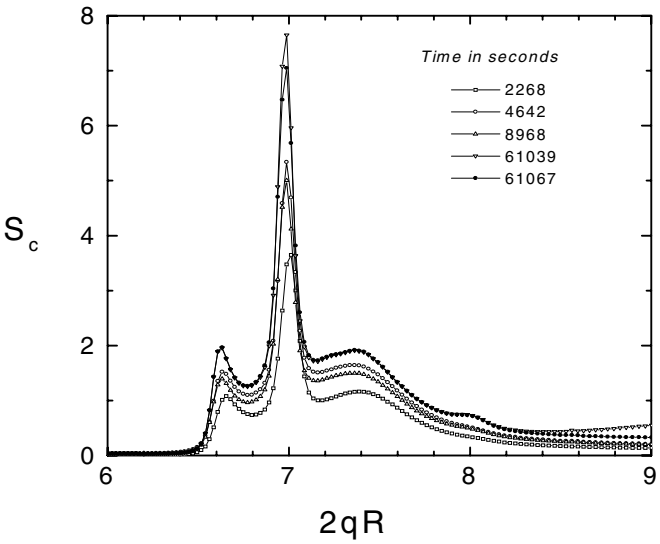

FIG. 1. The structure evolution of the sample with volume fraction $\phi = 0.528$. fcc {200} peak emerges during the crystal annealing with the equilibrium melting volume fraction $\phi_M = 0.545$ indicating fcc as the equilibrium crystal structure.

$$X(t) = c \int_{q_1}^{q_2} S_c(q, t) \quad (2)$$

with c a constant and the background excluded. The average linear dimension of the crystal (in units of the particle diameter $2R$) is given by

$$L(t) = \pi k/\Delta q(t)R, \quad (3)$$

where $k = 1.155$ is the Scherrer constant for a cubic shaped crystal. The number density of (average size) crystallites is estimated as

$$N_c(t) = X(t)/L^3(t). \quad (4)$$

Finally, the volume fraction $\phi_c(t)$ of a fcc (or any equivalently close-packed) crystal is related to the location of $q_m(t)$ of the {111} reflection using

$$\phi_c = \frac{2}{9\pi^2\sqrt{3}}[q_m(t)R]^3. \quad (5)$$

Several significant results were obtained experimentally. Simulations show that the fcc structure is most stable for ϕ near 0.7404, but just above melting, with $\phi \approx 0.545$, the situation is less clear [25,26]. A recent calculation coupled with simulations [27] found the entropy difference between fcc and hcp stackings to be 90.2 ± 4.3 in units of $10^{-5}k_B$ per sphere near melting, predicting the ground state to be fcc. Experiments on hard sphere colloidal crystals in normal gravity found a mixture of rhcp (random hexagonal close packing) and fcc with more rhcp [28]. The CDOT (colloidal disorder-order transition) experiment, which had less scattering angle resolution than PHaSE, showed the {200} fcc Bragg peak to be completely absent in microgravity and concluded that growth in microgravity yields almost pure rhcp crystals [16]. Here, as

shown in Fig. 1, we see the gradual growth of an fcc {200} peak at $2qR \sim 8$, beginning 3650 seconds after the initiation of crystallization when the liquid-to-crystal conversion has completed. This fcc peak continues to grow with time during the two week duration of the experiment. With increasing volume fraction ϕ, fcc shows up sooner [29]. Thus, we can conclude that fcc is the stable equilibrium structure for hard sphere crystals, but requires the very slow growth rates associated with annealing [30].

Figures 2(a)–2(d) presents the change in the average crystallite size, the number of crystallites, the total crystallinity, and the volume fraction of the crystalline and liquid phases, respectively, for $\phi = 0.528$. Several important conclusions follow.

Interaction between two crystallites: growth and coarsening.—One of the salient features, which has not been emphasized in previous experiments, is the existence of strong interactions between individual crystallites. In Fig. 2, from $t = 150$ s to about 800 s, the size of the crystallites increases linearly as $L = t^{\delta}$, $\delta = 0.99 \pm 0.05$, while the crystallinity X over this interval increases at a rate considerably less than L^3. Thus the number of crystallites decreases roughly as $N_c = t^{-\gamma}, \gamma = 2.6 \pm 0.2$. This is unusual and contrasts with the classic theory that focuses on the nucleation and growth in size of isolated crystallites. We identify this process as "simultaneous coarsening and growth" in which small crystallites shrink and eventually disappear, causing the number of crystallites to decrease, while large crystallites keep growing, causing the measured average crystallite size to increase with time. The growth exponent for the size is about unity, resulting from the combination of normal diffusion-limited growth and coarsening apparently due to direct transport from small to large crystallites [31]. Because of the different curvatures of these crystallites, the smaller crystallites are under higher pressure from the Laplace or surface tension term and hence have a high internal volume fraction value. Therefore, the corresponding equilibrium liquid volume fraction surrounding a small crystallite is relatively higher than that surrounding a large crystallite. Mass transport, via density gradients in the intervening fluid dispersion, moves particles from the small crystallites to the large crystallites.

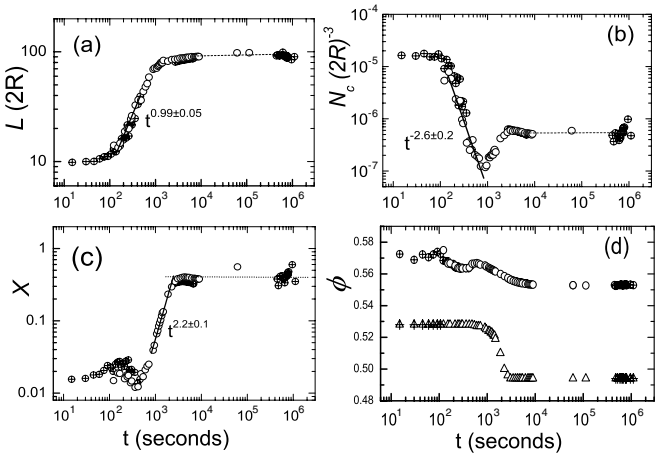

FIG. 2. Crystallization kinetics for a sample in the liquid-crystal coexistence region with $\phi = 0.528$. Shown are (a) average crystal size L, (b) number density of crystallites N_c, (c) crystallinity X, and (d) the volume fraction of spheres ϕ in crystal (circles) and liquid (triangles) phases as a function of time after shear melting. The STS-94 data are shown as symbols with + center and the STS-83 data are others.

Growth instability: dendrites.—This sample has a very distinctive feature. That is, at a late stage ($t > 800$ s), N_c increases again after rapidly decreasing during 100–800 s, as a consequence of the average crystallite size L changing only slightly, while the crystallinity X increases dramatically. In comparison, this phenomenon is totally absent in gravity (please refer to [32]) and cannot be interpreted as a nucleation process. We identify it as an instability in the diffusion-limited growth: dendritic crystal growth. Dendrites, the primary features of metal alloys, are of great technological importance and scientific interest. In colloidal systems, dendrites were first reported for charged colloids near a surface [33]; the CDOT experiment first observed hard sphere dendrites [16]. Figure 3 shows dendrites in all CDOT coexistence samples. The dendrites grown at $\phi = 0.52$ in a reflight of CDOT on the Mir Space Station remained intact with negligible or, at least, incomplete annealing after 2.5 months. In normal gravity fragile dendritic arms are prevented from growing by sedimentation [16] due to either viscous stresses on the crystallite or fluid flow that

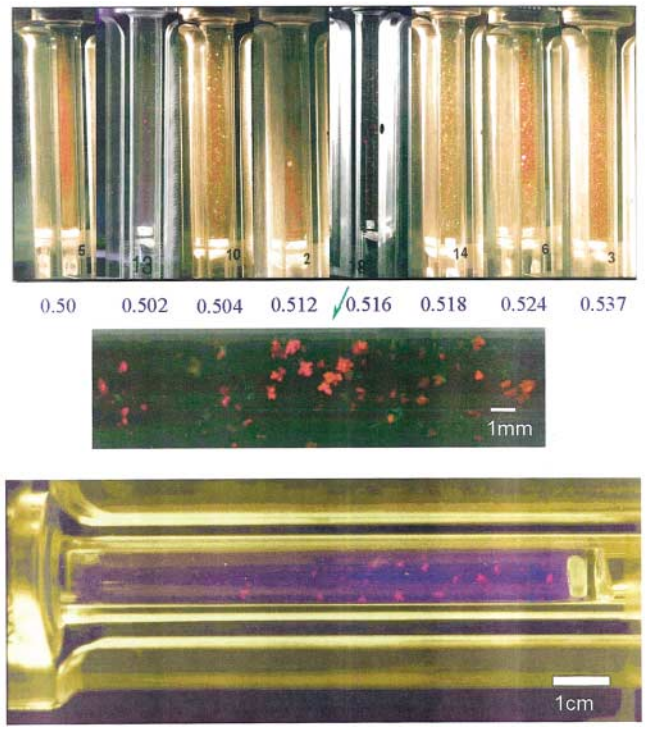

FIG. 3 (color). Photographs show the dendrites grown in CDOT samples with various volume fractions (top; middle inset: CDOT the second flight sample with $\phi = 0.516$) and in a sample with $\phi = 0.520$ on the Mir Space Station (bottom).

alters the diffusion field. Experiments on earth (without density matched samples) seldom observe the growth of dendrites.

A linear stability analysis [9] of hard sphere crystal growth indicates a dendritic instability at $\sim 13 r_c$ (r_c is the critical nucleus) for CDOT samples at $\phi = 0.504$, similar to the instability at $\sim 7 r_c$ in molecular systems [34]. Figure 2 suggests the critical nucleus to be about 10 times the diameter of the sphere. i.e., $r_c = 10 \times 2R$. At $t \approx 800$ s, the average crystallite size is about 70 times the diameter of the sphere, i.e., $r_{\text{crit}} = 70 \times 2R$. Therefore, the growth instability takes place at about $r_{\text{crit}} = 7 r_c$, which is in reasonable agreement with above-mentioned theoretical and experimental results.

We can also estimate other properties of the dendrites. Figure 2 shows that the apparent number density of the crystallites increases from $10^{-7}(2R)^{-3}$ to $6 \times 10^{-7}(2R)^{-3}$ from 800 to 3000 s. During this interval, L changes only slightly while the crystallinity X changes from 0.02 to 0.4, i.e., a 20-fold increase.

In a crude model we imagine that once the size surpasses r_{crit} further growth is predominantly from the dendritic arms. We then have

$$X \propto N_a N_c \rho^2 L_a \propto t^{2.2} \tag{6}$$

with the number of arms N_a, the arm radius ρ, and the arm length L_a. In this interpretation, the width of the (angle averaged) Bragg peak ($1/L$ in Fig. 2) is $\approx 1/\rho$, and ρ grows as a low power of time $\rho \sim L \sim t^{1/12}$. The maximum dendrite growth rate under marginal stability hypothesis is $dL_a/dt \propto 1/\rho$, then $L_a \propto t^{11/12}$. [This can also be obtained from mass conservation for the growing arm [9]: $(\phi_c - \phi_i)\frac{d}{dt}\rho^2 L_a = D\rho^2 \frac{(\phi_f - \phi_i)}{\rho}$, where ϕ_c, ϕ_f, ϕ_i are the volume fractions in the crystal, liquid, and at the interface, respectively, and D is the diffusion coefficient.] Combined with the equation above for X we have $N_a \propto t^{1.1}$. From $t_0 = 800$ s to $t_1 = 3000$ s, $X \approx (\rho_0^3 + N_a \rho^2 L_a)/\rho_0^3$ increases by 20 which gives the number of arms $N_a \sim 6$ at long times.

In summary, colloidal hard sphere crystallization has been studied without gravity. The fact that an fcc structure develops in microgravity as the samples anneal strongly suggests fcc to be the equilibrium phase for hard sphere crystals. The high density of crystallites affects the crystallization process quantitatively and qualitatively [32]. A picture with single crystallites growing in a metastable liquid significantly misses much of the kinetics that we have observed. A complete picture must involve the interaction between diffusion fields of the growing crystallites.

We are grateful to NASA for financial support and for the collaboration with the NASA PHaSE Tech Team and Space Shuttle Crews of STS-83 and STS-94.

*Present address: DiCon Fiberoptics Inc., 1689 Regatta Boulevard, Richmond, California 94804.
Email address: zcheng@diconfiber.com

[1] J. P. Hansen and I. R. McDonald, *Theory of Simple Liquids* (Academic Press, New York, 1986), 2nd ed.
[2] P. N. Pusey, in *Liquid, Freezing and the Glass Transition,* edited by J. P. Hansen, D. Levesque, and J. Zinn-Justin (Elsevier, Amsterdam, 1991), Chap. 10.
[3] W. van Megen and P. N. Pusey, Phys. Rev. A **43**, 5429 (1991).
[4] W. van Megen and S. M. Underwood, Phys. Rev. Lett. **70**, 2766 (1993).
[5] W. Götze, in *Liquid, Freezing and the Glass Transition* (Ref. [2]), Chap. 5.
[6] S.-E. Phan *et al.,* Phys. Rev. E **54**, 6633 (1996).
[7] W. B. Russel, Phase Transit. **21**, 27 (1990).
[8] B. J. Ackerson and K. Schätzel, Phys. Rev. E **52**, 6448 (1995).
[9] W. B. Russel *et al.,* Langmuir **13**, 3871 (1997).
[10] T. Palberg, J. Phys. Condens. Matter **11**, R323 (1999).
[11] K. Schätzel and B. J. Ackerson, Phys. Rev. Lett. **68**, 337 (1992).
[12] K. Schätzel and B. J. Ackerson, Phys. Rev. E **48**, 3766 (1993).
[13] Y. He *et al.,* Phys. Rev. E **54**, 5286 (1986).
[14] J. L. Harland and W. van Megen, Phys. Rev. E **55**, 3054 (1997).
[15] J. L. Harland *et al.,* Phys. Rev. Lett. **75**, 3572 (1995).
[16] J. Zhu, M. Li, R. Rogers, W. Meyer, R. H. Ottewill, STS-73 Space Shuttle Crew, W. B. Russel, and P. M. Chaikin, Nature (London) **387**, 883 (1997).
[17] Z. Cheng *et al.,* Mater. Des. **22**, 529 (2001).
[18] C. T. Lant, A. E. Smart, D. S. Cannell, W. V. Meyer, and M. P. Doherty, Appl. Opt. **36**, 7501 (1997).
[19] S.-E. Phan *et al.,* Phys. Rev. E **60**, 1988 (1999).
[20] http://zeta.lerc.nasa.gov/phase/
[21] L. Verlet and J. J. Weis, Phys. Rev. A **5**, 939 (1972).
[22] J. C. Wilson, Proc. R. Soc. London A **180**, 277 (1942).
[23] W. Loose and B. J. Ackerson, J. Chem. Phys. **101**, 7211 (1994).
[24] G. W. Brindley and J. Méring, Acta Crystallogr. **4**, 441 (1951).
[25] D. Frenkel and A. J. C. Ladd, J. Chem. Phys. **81**, 3188 (1984).
[26] L. V. Woodcock, Nature (London) **385**, 141 (1997).
[27] S. C. Mau and D. A. Huse, Phys. Rev. E **59**, 4396 (1999).
[28] P. N. Pusey *et al.,* Phys. Rev. Lett. **63**, 2753 (1989).
[29] Z. Cheng, J. Zhu, W. B. Russel, W. V. Meyer, and P. M. Chaikin, Appl. Opt. **40**, 4146 (2001).
[30] S. Pronk and D. Frenkel, J. Chem. Phys. **110**, 4589 (1999).
[31] C. Sagui, D. S. O'Gorman, and M. Grant, Phys. Rev. E **56**, R21 (1997).
[32] Z. Cheng, Ph.D. thesis, Princeton University, 1998.
[33] A. Gast and Y. Monovoukas, Nature (London) **351**, 553 (1991).
[34] J. S. Langer, Rev. Mod. Phys. **52**, 1 (1980).